Deep Learning System to Screen Coronavirus Disease

Dr.K.Venkata Nagendra#1, Mr.G.Rajesh#2,

Dr.MaligelaUssenaiah#3

#1 Associate Professor,Department of CSE, Audisankara College of Engineering & Technology, Gudur.

#2 Assistant Professor, Department of CSE, Audisankara College of Engineering & Technology, Gudur.

#3 Assistant Professor, Department of CS, VikramaSimhapuri University, Nellore.

ABSTRACT

We discovered that the ongoing converse interpretation polymerase chain response (RT-PCR) identification of viral RNA from sputum or nasopharyngeal swab has a moderately low positive rate in the beginning time to decide COVID-19 (named by the World Health Organization). The signs of figured tomography (CT) imaging of COVID-19 had their own qualities, which are unique in relation to different sorts of viral pneumonia, for example, Influenza-A viral pneumonia. Accordingly, clinical specialists require another early demonstrative criteria for this new sort of pneumonia as quickly as time permits.

OBJECTIVE: This examination intended to build up an early screening model to recognize COVID-19 pneumonia from Influenza-A viral pneumonia and sound cases with aspiratory CT pictures utilizing profound learning procedures.

1. INTRODUCTION

At the end of 2019, the novel coronavirus disease 2019 pneumonia (COVID-19) occurred in the city of Wuhan, China.[1-4] On January 24, 2020, Huang et al.[5] summarized the clinical characteristics of 41 patients with COVID-19, indicating that the common onset symptoms were fever, cough, myalgia, or fatigue. All these 41 patients had pneumonia and their chest CT examination showed abnormalities. The complications included acute respiratory distress syndrome, acute heart injury, and secondary infections. Thirteen (32%) patients were admitted to the intensive care unit (ICU), and six (15%) died. The the Kok-KH[6] team at the University of Hong Kong found the evidence of human-to-human transmission of COVID-19 for the first time.

COVID-19 causes severe respiratory symptoms and is associated with relatively high ICU admission and mortality. The current clinical experience for treating these patients revealed that the RT-PCR detection of viral RNA from sputum or nasopharyngeal swab had a low positive rate in the early stage. However, a high proportion of abnormal chest CT images were obtained from patients with this disease. The manifestations of CT imaging of COVID-19 cases had their own characteristics, different from the manifestations of CT imaging of other viral pneumonia such as Influenza-A viral pneumonia, as showed in Figure 1. Therefore, clinical doctors called for replacing nucleic acid testing with lung CT as one of the early diagnostic criteria for this new type of pneumonia as soon aspossible.With the rapid development of computer technology, digital image processing technology has been widely applied in the medical field, including organ segmentation and image enhancement and repair, providing support for

subsequent medical diagnosis.[7,8] Deep learning technologies, such as convolutional neural network (CNN) with the strong ability of nonlinear modeling, have extensive applications in medical image processing as well.[9-12] Relevant studies were conducted on the diagnosis of pulmonary nodules,[13-14] classification of benign and malignant tumors,[15] and pulmonary tuberculosis analysis and disease prediction[16-18]worldwide.

In this study, multiple CNN models were used to classify CT image datasets and calculate the infection probability of COVID-19. The findings might greatly assist in the early screening of patients with COVID-19.

2. METHOD

2.1 Datasetintroduction

A total of 618 transverse-section CT samples were collected in this study, including 219 from 110 patients with COVID-19 from the First Affiliated Hospital of Zhejiang University, the No.6 People's Hospital of Wenzhou, and the No.1 People's Hospital of Wenling, from Jan 19 to Feb 14, 2020. All three hospitals are designated COVID-19 hospitals in Zhejiang Province. Every COVID-19 patient was confirmed with RT-PCR testing kit and we also excluded the cases that had no image manifestations on the chest CT images. In addition, there had at least two days gap between CT datasets iftaken from the same patient to ensure the diversity of samples. The remaining 399 CT samples were collected from the First Affiliated Hospital of Zhejiang University as the controlled experiment group. Among them, 224 CT samples were from 224 patients with Influenza-A viral pneumonia including H1N1, H3N2, H5N1, H7N9 etc., and175CTsamplesfromhealthypeople.Therewere198(90.4%)COVID-19and (196) 86.6% Influenza-A cases from early or progressive stages and the rest 9.6% and 13.4% cases from severe stage respectively ($P > 0.05$). Moreover, Influenza-A viral pneumonia CT cases used as it was most critically to distinguish them from suspected patients with COVID-19 currently in China.

The ethics committee of the First Affiliated Hospital, College of Medicine, Zhejiang University approved this study and all research was performed in accordance with relevant guidelines/regulations. All participants and/or their legal guardians signed the informed consent form before the study.

A total of 528 CT samples (85.4%) were used for training and validation sets, including 189 samples of patients with COVID-19, 194 samples from patients with Influenza-A viral pneumonia, and 145 samples from healthy people. The remaining 90 CT sets (14.6%) were used as the test set, including 30 COVID-19, 30 Influenza-A viral pneumonia, and 30 healthy case. Furthermore, the test cases of CT set were selected from the people who had not been included in the trainingstage.

(a) (b) (c)

Figure 1. Typical transverse-section CT images: (a) COVID-19; (b) Influenza-A viral pneumonia; (c) no pneumonia manifestations on this chest CT image.

2.2 Process

Figure 2 shows the whole process of COVID-19 diagnostic report generation in this study. First, the CT images were preprocessed to extract effective pulmonary regions. Second, a 3D CNN model was used to segment multiple candidate image cubes. The center image, together with the two neighbors of each cube, was collected for further steps. Third, an image classification model was used to categorize all the image patches into three types: COVID-19, Influenza-A-viral-pneumonia, and irrelevant-to-infection. Image patches from the same cube voted for the type and confidence score of the candidate as a whole. Finally, the overall analysis report for one CT sample was calculated using the Noisy-or Bayesian function.[19]

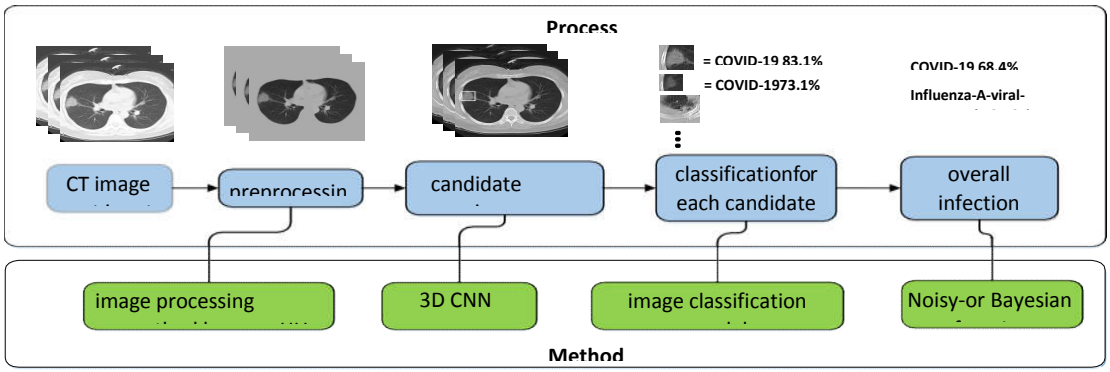

Figure 2.Process flow chart.

2.3 Dataset preprocessing and candidate regionsegmentation

To study was expedited using the same method and models in data preprocessing and candidate region segmentation stages as a previous study on pulmonary tuberculosis.[17] The focus of infections from pulmonary tuberculosis had multiple structures and types, including miliary, infiltrative, caseous, tuberculoma, and cavitary

etc. Although, the VNET[20] based segmentation model VNET-IR-RPN[17]was trained for pulmonary tuberculosis purpose, it was verified to be still good enough to separate candidate patches from viralpneumonia.

Moreover, in the study of pulmonary tuberculosis, the VNET-IR-RPN model was used both for both segmentation and classification. Only the segmentation-related bounding box regression part was preserved, regardless of the classification results, because only the former task was required at this stage in this study.

2.4 Image data processing andaugmentation

A large number of non-infection regions irrelevant to this study were also separated using the 3D segmentation model, including fibrotic structure of pulmonary, calcification spots, or healthy regions identified incorrectly. Therefore, an extra category was added as irrelevant-to-infection besides COVID-19 and Influenza-A-viral-pneumonia.

The study included 618 CT samples (219 COVID-19, 224 Influenza-A-viral-pneumonia, and 175 healthy case). Subsequently, a total of 3957 candidate cubes were generated from the 3D segmentation model. Only the territory close to the middle of this cube contained maximum information about this focus of infection. Hence, only the center image together with the two neighbors of each cube was collected to represent this region for future classification steps. Next, all image patches were manually classified by two professional radiologists into two types: irrelevant-to-infection and pneumonia. The the images in the latter category were recognized automatically as COVID-19 or Influenza-A-viral-pneumonia based on the clinical diagnosis results.A total of 11,871 image patches were acquired from the aforementioned steps, including 2,634 COVID-19, 2,661 Influenza-A-viral-pneumonia, and 6,576 irrelevant-to-infection. According to the previous dataset assignment, the training and validation sets had 528 CT samples, equivalent to 10,161 (85.6%) images, including 2,301 COVID-19, 2,244 Influenza-A-viral-pneumonia, and 5,616irrelevant-to-infection images. The remaining 1,710 (14.4%) images were reservedforthe test dataset.The sampling possibility of COVID-19 and Influenza-A-viral-pneumonia cases was expanded three times to balance the specimen number of irrelevant-to-infection so as to reduce the influence of the uneven distribution of different image types on the present dataset. At the same time, generic data expansion mechanisms, such as random clipping, left-right, up-down flipping, and mirroring operation, were performed on specimens to increase the number of training samples and prevent data overfitting.

3. RESULTS

3.1 Evaluationplatform

An Intel i7-8700k CPU together with NVIDIA GPU GeForce GTX 1080ti was used as the testing server. The processing time largely depended on the number of image layers in one CT set. On average, it was less than 30s for a CT set with 70 layers from data-preprocessing to the output of thereport.

3.2 Trainingprocess

As one of the most classical loss function used in classification models, cross-entropy was used in this study. When the epoch number of training iterations increased to more than 1000, the loss value did not decrease or increase obviously, suggesting that the

models converged well to a relative optimal state without distinct overfitting. The training curves of the loss value and the accuracy for two classification models were showed in Figure 3. The network with the location-attention mechanism achieved better performance on the training dataset compared with the originalResNet.

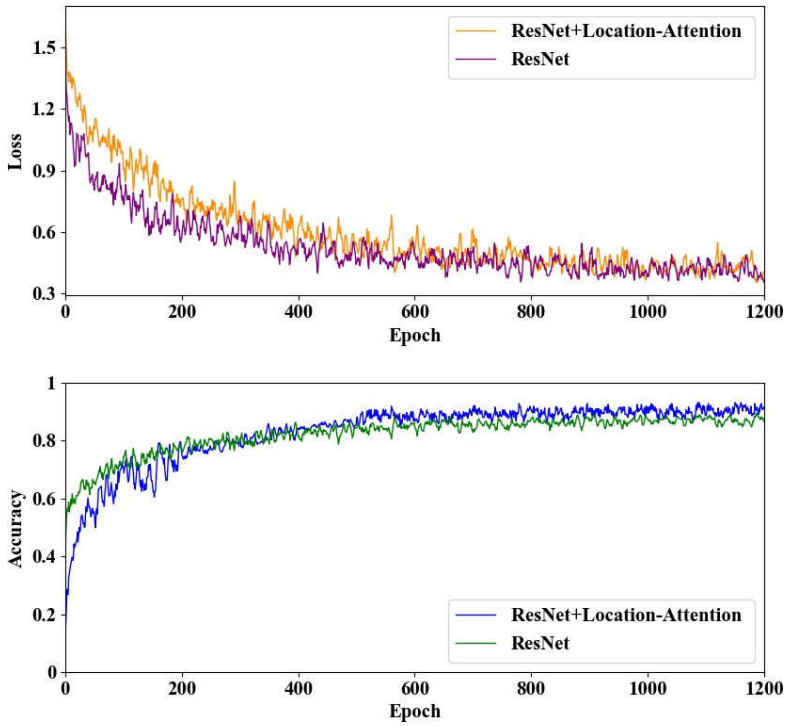

Figure 3.Training curve of loss and accuracy for the two classification models.

3.3 Performance on testdataset

3.3.1 Performancemeasurement

The *accuracy* of a method determines how correct the values are predicted. *Precision* determines the reproducibility of the measurement or how many of the predictions are correct. *Recall* shows how many of the correct results are discovered. *F1-score* uses a combination of precision and recall to calculate a balanced average result. The following equations show how to calculate these values, where TP, TN, FP and FN aretrue positive, true negative, false positive, and false negative respectively.

3.3.2 Segmentation

A total of 30 CT samples were selected randomly from each group (COVID-19, Influenza-A-viral-pneumonia and healthy) for the test set, following the rule that this person (owner of this CT) had not been included in the previous training stage. Moreover, the segmentation model VNET-IR-RPN was configured to reduce the proposal's threshold to maximum separate candidate regions even through many normal regions could be included in. One CT case from COVID-19 group that had no region segmented as COVID-19 or Influenza-A-viral-pneumonia and hence wrongly categorized into the no-infection-found group, as showed in Figure 4. These focus ofinfections could be barely notified by human eyed and seemed too tenuous to be captured by the segmentation model for this study.

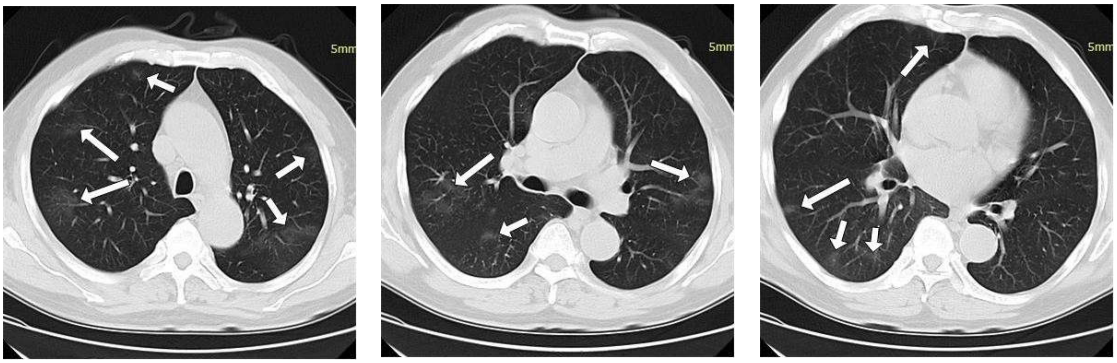

(a) (b) (c)

Figure 4.All CT images from a single CT case. The focus of infections are pointed out by arrows.

3.3.3 Classification for a single imagepatch

A total of 1,710 image patches were acquired from 90 CT samples, including 357 COVID-19, 390 Influenza-A-viral-pneumonia, and 963 irrelevant-to-infection (ground truth). To determine which was the optimal approach, the design of each methodology was assessed using a confusion matrix. Two network structures were evaluated: with and without the location-attention mechanism, as showed in Table 1 and Table2.

		Predicted result		
		COVID-19 (M_1/M_2)	IAVP (M_1/M_2)	ITI (M_1/M_2)
Actual result	COVID-19 (M_1/M_2)	260/273	47/32	50/52
	IAVP (M_1/M_2)	55/46	276/280	59/64
	ITI (M_1/M_2)	75/77	81/82	807/804

Table 1. The confusion matrix of COVID-19, Influenza-A-viral-pneumonia (IAVP) and irrelevant-to-infection (ITI). M1 and M2 referred to ResNet model and ResNet with location-attention mechanism model.

	Recall (M_1,M_2)	Precision (M_1,M_2)	f1-score (M_1,M_2)
COVID-19 (M_1,M_2)	0.728/0.765	0.667/0.689	0.696/0.725
IAVP (M_1,M_2)	0.708/0.718	0.683/0.711	0.695/0.714
ITI (M_1,M_2)	0.838/0.835	0.881/0.874	0.859/0.854

Table 2. The recall, precision and f1-score of two classification models for COVID-19, Influenza-A-viral-pneumonia (IAVP) and irrelevant-to-infection (ITI). M1 and M2 referred to ResNet model and ResNet with location-attention mechanism model.

The average f1_scores for two models were 0.750 and 0.764, which indicated that the second model with location-attention mechanism achieved better performance averagely. Therefore, this model was used for the rest of this study.

3.3.4 Vote for aregion

Each image patch voted to represent this entire candidate region. A total of 570 candidate cubes were distinguished, including 119COVID-19, 130 Influenza-A-viral-pneumonia and 321 irrelevant-to-infection regions (ground truth). The confusion matrix of voting result and corresponding recall, precision and f1-score were showed in Table 3 and Table 4. The average f1-score for three categories was 0.856 and had an improvement of 12.1% compared with previous step.

Predicted result				
		COVID-19	IAVP	ITI
Actual result	COVID-19	97	15	7
	IAVP	18	98	14
	ITI	5	2	314

Table3. The confusion matrix of COVID-19, Influenza-A-viral-pneumonia (IAVP) and irrelevant-to-infection(ITI).

		Recall	Precision	f1-score
Actual result	COVID-19	0.815	0.808	0.811
	IAVP	0.754	0.852	0.800
	ITI	0.978	0.937	0.957

Table 4. The recall, precision and f1-score of after voting process for each regions: COVID-19, Influenza-A-viral-pneumonia (IAVP) and irrelevant-to-infection (ITI).

3.3.5 Result of the classification for the CT samples as awhole

Noisy-or Bayesian function was used to identify the dominated infection types. Three types result exported in the final report: COVID-19, Influenza-A-viral-pneumonia and no-infection-found. The experimental results are summarize in Table 5 and Table 6. As the irrelevant-to-infection items (previous step) would be ignored and not be counted by the Bayesian function, we only compare the average f1-score for the first two items. They were 0.806 and 0.843 respectively, which showed a promotion of 4.7%. Moreover, the overall classification accuracy for all three groups are86.7%.

Predicted result COVID-19			IAVP	NIF
Actual result	COVID-19	26	3	1
	IAVP	4	25	1
	NIF	2	1	27

Table5. The confusion matrix of COVID-19, Influenza-A-viral-pneumonia (IAVP) and no-infection-found (NIF).

		Recall	Precision	f1-score
Actual result	COVID-19	0.867	0.813	0.839
	IAVP	0.833	0.862	0.847
	NIF	0.900	0.931	0.915

Table 6. The recall, precision and f1-score from the output of the Bayesian function for COVID-19, Influenza-A-viral-pneumonia (IAVP) and no-infection-found (NIF).

5. DISCUSSION

COVID-19, which was first recognized in Wuhan China, has caused certified general prosperity security issues and therefore become an overall concern.25-27 The extraordinary situation progresses new requirements for the shirking and control procedure. Endless patients with viral pneumonia had been perceived in Wuhan city. The RT-PCR preliminary of 2019-nCoV RNA can make an unequivocal finding of COVID-19 from Influenza-A viral pneumonia patients. In any case, the nucleic destructive testing has a couple of disfigurements, for instance, time slack, respectably low area rate, and short of supply. In the first place time of COVID-19, a couple of patients may starting at now have positive aspiratory imaging disclosures anyway they have no sputum and negative test realizes nasopharyngeal swabs of RT-PCR. These patients are not broke down as suspected or avowed cases. Right now, are not be isolated or treated on the grounds that, making them potential wellsprings of infection.

The CT imaging of COVID-19 present a couple of specific signs according to past studies.21,22 The appearances consolidate focal ground glass shadows fundamentally scattered in complementary lungs, different cementing shadows joined by the "brilliance sign" of incorporating ground glass shadow in the two lungs, work shadows and bronchiectasis and exploding signs inside the injuries, and various mix of different sizes and network formed high-thickness shadows. In any case, it isn't objective and definite to perceive COVID-19 from various diseases just with human eyes. In assessment, significant learning structure based screen models revealed logically express and trustworthy results by digitizing and regulating the image information. From this

time forward, they can help specialists to choose a smart clinical decision even more unequivocally, which would benefit on the leading group of suspected patients.

At the present time, significant learning development was used to design a course of action sort out for perceiving the COVID-19 from Influenza-A viral pneumonia. To the extent the framework structure, the old style ResNet was used for feature extraction. It was differentiated and the framework model with and without the extra region thought instrument. The preliminary showed that the recently referenced instrument could all the more promptly perceive COVID-19 cases from others.

The sign of COVID-19 may have some spread with the appearances of changed pneumonias, for instance, Influenza-A viral pneumonia, characteristic pneumonia and eosinophilic pneumonia. The clinical examination of COVID-19 needs to join the patients' contact history, travel history, first reactions and research office evaluation. At this moment, number of model models was compelled. Thusly, the arrangement and test the amount of tests should be develop to improve the accuracy later on. More multi-center clinical examinations should be directed to adjust to the complex clinical situation. Furthermore, tries should be made to improve the division and request model. A better select models should than be expected for setting up, the division and gathering precision of the model should be improved, and the hypothesis execution of this count should be affirmed with a greater instructive assortment.

4. CONCLUSION

In this multi-center case study, we had presented a novel method that could screen COVID-19 fully automatically by deep learning technologies. Models with location-attention mechanism could more accurately classify COVID-19 at chest radiography with the overall accuracy rate of 86.7 % and could be a promising supplementary diagnostic method for frontline clinical doctors.

References

1. Zhu N, Zhang D, Wang W, et al. A Novel Coronavirus from Patients with Pneumonia in China, 2019[J]. N Engl J Med. 2020 Jan 24. doi: 10.1056/NEJMoa2001017.
2. Li Q, Guan X, Wu P, et al. Early Transmission Dynamics in Wuhan, China, of Novel Coronavirus-Infected Pneumonia[J]. N Engl J Med. 2020 Jan 29. doi: 10.1056/NEJMoa2001316.
3. CohenJ,NormileD.NewSARS-likevirusinChinatriggersalarm[J].Science.2020 Jan 17; 367(6475):234-235. doi: 10.1126/science.367.6475.234.
4. Corman VM, Landt O, Kaiser M, et al. Detection of 2019 novel coronavirus (2019-nCoV) by real-time RT-PCR[J].Euro Surveill. 2020 Jan; 25(3). doi: 10.2807/1560-7917.ES.2020.25.3.2000045.
5. Huang C, Wang Y, Li X, et al. Clinical features of patients infected with 2019 novel coronavirus in Wuhan, China[J]. Lancet. 2020 Jan 24. pii: S0140-6736(20)30183-5.doi:10.1016/S0140-6736(20)30183-5.
6. Chan JF, Yuan S, Kok KH, et al. A familial cluster of pneumonia associated with the 2019 novel coronavirus indicating person-to-person transmission: a study of a family cluster[J]. Lancet. 2020 Jan 24. pii: S0140-6736(20)30154-9. doi:

10.1016/S0140-6736(20)30154-9.
7. Liu X, Guo S, Yang B, et al. Automatic Organ Segmentation for CT Scans Based on Super-Pixel and Convolutional Neural Networks[J]. Journal of Digital Imaging, 2018,31(6).
8. Gharbi, Michaël, Chen J, Barron J T, et al. Deep Bilateral Learning for Real - Time Image Enhancement[J]. Acm Transactions on Graphics, 2017,36(4):118.
9. Hesamian M H, JiaW, He X, et al. Deep Learning Techniques for Medical Image Segmentation: Achievements and Challenges[J]. Journal of Digital Imaging, 2019, 32(8).
10. Akagi M, Nakamura Y, HigakiT, et al. Correction to: Deep learning reconstruction improves image quality of abdominal ultra-high-resolution CT[J]. European Radiology, 2019,29(8).
11. NardelliP, Jimenez-Carretero D, Bermejo-Pelaez D, et al. Pulmonary Artery-Vein Classification in CT Images Using Deep Learning[J]. IEEE Transactions on Medical Imaging, 2018,PP(99):1-1.
12. Zhu W, Huang Y, ZengL, et al. AnatomyNet: Deep learning for fast and fully automated whole-volume segmentation of head and neck anatomy[J]. Medical Physics, 2019,46(2).
13. Huang P, Park S, Yan R, et al. Added Value of Computer-aided CT Image Features for Early Lung Cancer Diagnosis with Small Pulmonary Nodules: A Matched Case-Control Study. Radiology.2018 Jan; 286(1):286-295. doi: 10.1148/radiol.2017162725.

Author's Profiles

Dr.K.VenkataNagendra, working as Associate Professor in the Department of Computer Science Engineering at Audisankara College of Engineering & Technology, Gudur, Nellore Dt, Andhra Pradesh, India. He has 10 years of experience in the field of teaching. He got doctorate from VikramaSimhapuri University. He did his M.Tech in ANU, Guntur. His areas of interests are Data warehousing and Data Mining, Machine Learning and Deep Learning.

Mr.G.Rajesh working as Assistant Professor in the Department of Computer Science Engineering at Audisankara College of Engineering & Technology, Gudur, Nellore Dt, Andhra Pradesh, India. He has 10 years of experience in the field of teaching. He is a research scholar in Rayalaseema University, Kurnool. He did his M.Tech in JNTU, Hyderabad. His areas of interests are Data warehousing and Data Mining and Computer Network.

Dr.MaligelaUssenaiah, working as Assistant Professor in the Department of Computer Science in VikramaSimhapuri University, Nellore, Andhra Pradesh, India. He is having 10 years of teaching experience. He did his PhD in Computer Science from SriKrishnaDevarayaUniveristy, Ananthapur, Andhra Pradesh. His areas of interests are Networks, Mobile Wireless Networks, Data warehousing and Data Mining and Image processing.